

Jan Chleboun

On a Sandia structural mechanics challenge problem

In: Jan Chleboun and Karel Segeth and Tomáš Vejchodský (eds.): Programs and Algorithms of Numerical Mathematics, Proceedings of Seminar. Prague, May 28-31, 2006. Institute of Mathematics AS CR, Prague, 2006. pp. 53–59.

Persistent URL: <http://dml.cz/dmlcz/702818>

Terms of use:

© Institute of Mathematics AS CR, 2006

Institute of Mathematics of the Czech Academy of Sciences provides access to digitized documents strictly for personal use. Each copy of any part of this document must contain these *Terms of use*.



This document has been digitized, optimized for electronic delivery and stamped with digital signature within the project *DML-CZ: The Czech Digital Mathematics Library*
<http://dml.cz>

ON A SANDIA STRUCTURAL MECHANICS CHALLENGE PROBLEM*

Jan Chleboun

1. Introduction

A structural mechanics prediction problem was proposed by Ivo Babuška, Fabio Nobile, and Raul Tempone as one of the uncertain input data problems specially designed to challenge the participants of Validation Challenge Workshop, Sandia National Laboratories, Albuquerque, NM, USA, May 21-23, 2006; see [1].

The prediction problem concerns the structure sketched in Figure 1 (left), the coordinates of the joints are given in meters. The rods are joined by pins (zero moment connections) at the junctions and hinges. The horizontal beam (number 4 in Figure 1 (left)) is loaded by a uniform force. The vertical displacement of P , the midpoint of the horizontal beam, is denoted by δ_P and exaggerated. Since the force acts downward, δ_P is negative; we refer to [1], where $w(P_m) \equiv \delta_P$, for details.

The prediction problem is posed as follows: What is the probability that $\delta_P \geq -3$ mm? Or, in a broader sense: How can we assess the occurrence of the $\delta_P \geq -3$ mm phenomenon?

The difficulty of the problem lies in limited information about material parameter E , the modulus of elasticity (Young modulus) of the truss structure members. The material of the bars and the beam is represented by the Young modulus that is assumed to be a homogeneous random field. The modulus and its probabilistic properties are not known and have to be inferred and characterized from available data. In [1], three embedded sets of data are presented. In this analysis, we confine ourselves to the first, most limited dataset.

It comprises: a vector $E_0^v = (13.26, 10.86, 14.77, 10.94, 11.05)$ of five local values of E in GPa, see the top five values in the third column of [1, Table 6]; a vector $E_{20}^v = (11.65, 11.21, 11.45, 10.89, 11.67)$ of five averaged values of E (in GPa) inferred from the elongation of sample rods 20 cm long (calibration experiments; cross-section area $A = 4$ mm², force $F = 1200$ N), see the top five values in the second column of [1, Table 6] for the elongations; a vector $E_{80}^v = (11.94, 11.65)$ of two averaged values of E (in GPa) inferred from the elongation of sample rods 80 cm

*This research was supported by the Czech Science Foundation, grant 201/04/1503, and by the Academy of Sciences of the Czech Republic, Institutional Research Plan No. AV0Z10190503. The author thanks Ivo Babuška, Fabio Nobile, and Raul Tempone for fruitful discussions about the challenge problem, and Ivan Saxl for valuable comments on an earlier version of the manuscript.

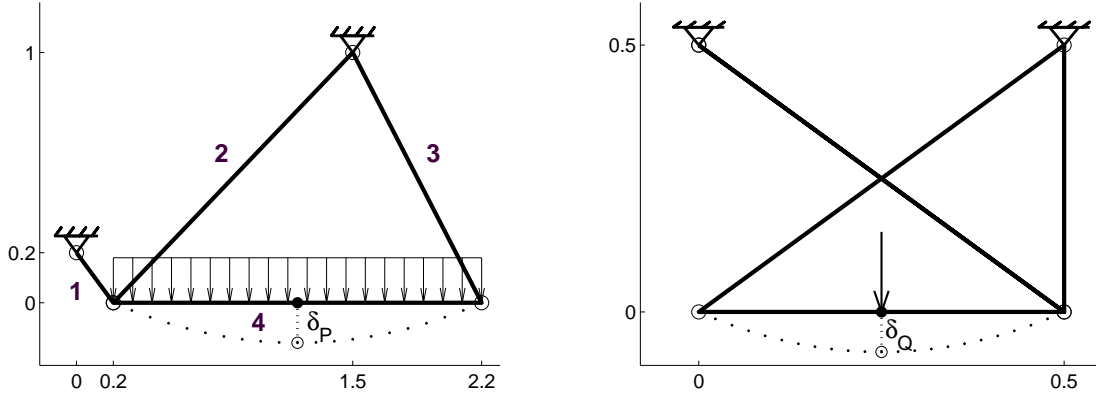


Fig. 1: Prediction problem (left). Accreditation experiment (right).

long (validation experiments; $A = 4 \text{ mm}^2$, $F = 1200 \text{ N}$), see the top two values in the second column of [1, Table 7]; and δ_Q , a particular displacement observed in a “similar”, point-loaded structure in an *accreditation experiment* [1], see Figure 1 (right) and the first value of $w(P)$ (correctly $w(Q)$) in [1, Table 8]. Vectors E_0^v , E_{20}^v , and E_{80}^v stem from sampling random variables E_0 , E_{20} , and E_{80} , respectively.

The geometry of the structures as well as of the individual bars and beams is exactly known. The structures are statically determined, therefore the load-to-displacement mapping can be expressed by an explicit formula, see [1] for details.

2. Analysis

The probability distribution of the Young modulus value is unknown. The number of measurements is not sufficient to allow for strong results of a statistical analysis; the estimates of probability related parameters would be poor. Nevertheless, a stochastic-based approach will be used to tackle the uncertainty problem.

Let us identify the longitudinal axis of each rod with a local coordinate system axis in such a way that the left end of the rod coincides with the origin. Along each rod, the Young modulus is supposed to be a stationary random field, $E(x)$, where $x \in [0, L]$ and L is the length of the rod. Some features of this field are assumed to be independent of x . For example, $\mathbf{E}(E(x))$, the expected value of the Young modulus at point x , is assumed to be constant and independent of x and of a particular choice of the rod; similarly for higher statistical moments. This is why we can identify $E(x)$ with an x -independent random variable E_0 in certain analyses.

We have to assume that $E(x_1)$ and $E(x_2)$ are not mutually independent, especially if x_1 is “close” to x_2 . In other words, $E(x_1)$ and $E(x_2)$ are correlated. However, the formula representing the model of correlation is not known. We will *assume* a formula dependent on one parameter, called correlation length, that has to be determined from the available data.

The method of treating the prediction problem can be summarized as follows:

- Choose respective intervals I_0 and I_{20} that exceed the range of the measured values E_0^v and E_{20}^v . These intervals represent the assumed range of random variables E_0 and E_{20} .
- Assume a probability distribution of E_0 and E_{20} (uniform or normal).
- For $1/E$, assume a covariance function with an unknown correlation length L_{corr} .
- By using the assumptions, calculate the correlation length L_{corr} .
- By knowing L_{corr} , infer I_{80} , an interval representing the range of the random variable E_{80} , and check it against E_{80}^v . It is assumed that E_{80} retains the probability distribution of E_0 and E_{20} (uniform or normal).
- By knowing L_{corr} , infer an interval representing the range of the random variable δ_Q and check it against the value of δ_Q coming from the accreditation experiment.
- By knowing L_{corr} , infer an interval representing the range of δ_P and check it against the -3 mm limit given in the prediction problem. Try to make a conclusion.

Inevitably, expert opinion is required to make realistic assumptions needed in the above-listed steps.

The intervals I_0 and I_{20} are constructed to have a common center. They are interpreted as either the respective intervals in which both E_0 and E_{20} are uniformly distributed (i.e., E_0 and E_{20} do not exceed I_0 and I_{20} , respectively), or the intervals covering 95% of normally distributed values E_0 and E_{20} (i.e., the probability that these random quantities leave their intervals is 0.05). The normal distribution assumption can be challenged because normally distributed values of E would allow for a negative Young moduli (with a low probability), which is physically impossible.

We have a double reason for using the normal distribution. First, we wish to compare the results obtained for the uniform probability distribution with the results obtained for a non-uniform distribution. Second, we wish to minimize the use of numerical methods, which is possible for the above-mentioned distributions. Moreover, the normal distribution assumption may still be adequate for understanding the dominant behavior of the rods and structures.

Let us recall that E_0 is a random field of local values of E , that is, a field identical to $E(x)$ except for the localization at a particular x .

We assume that the covariance function of $1/E$ is related to the variance of $1/E$ in a particular way mediated through an L_{corr} -dependent function (cf. [2, Example 1]):

$$\text{cov}[1/E(x_1), 1/E(x_2)] = \text{var}(1/E_0) \exp(-|x_1 - x_2|/L_{\text{corr}}). \quad (1)$$

If a bar of length L and cross-section area A is axially loaded by a force F , then for δ_L , its elongation, holds

$$\delta_L = \frac{F}{A} \int_0^L \frac{1}{E(x)} dx. \quad (2)$$

Since $E(x)$ is a random variable, δ_L is a random variable, too.

By (2) used in $\text{var}(\delta_L) = \mathbf{E}[\delta_L^2] - (\mathbf{E}[\delta_L])^2$ and by (1), we infer

$$\begin{aligned}\text{var}(\delta_L) &= \frac{F^2}{A^2} \int_0^L \int_0^L \left\{ \mathbf{E}[1/E(x_1), 1/E(x_2)] - (\mathbf{E}[1/E_0])^2 \right\} dx_1 dx_2 \\ &= \frac{F^2}{A^2} \int_0^L \int_0^L \text{cov}[1/E(x_1), 1/E(x_2)] dx_1 dx_2 \\ &= \frac{F^2}{A^2} \text{var}(1/E_0) \int_0^L \int_0^L \exp\left(-\frac{|x_1 - x_2|}{L_{\text{corr}}}\right) dx_1 dx_2.\end{aligned}\quad (3)$$

If we define E_L as the *effective* modulus of elasticity inferred from the prolongation of the bar of length L via the equality $\delta_L = FL/(AE_L)$, then E_L is also a random variable and its variance can be calculated as $\text{var}(\delta_L) = \text{var}(1/E_L)F^2L^2/A^2$. By this equality combined with (3), we eliminate $\text{var}(\delta_L)$ and obtain

$$\frac{\text{var}(1/E_L)}{\text{var}(1/E_0)} = \frac{1}{L^2} \int_0^L \int_0^L \exp\left(-\frac{|x_1 - x_2|}{L_{\text{corr}}}\right) dx_1 dx_2.\quad (4)$$

To solve (4), we evaluate $\text{var}(1/E_0)$ stemming from the assumed probability distribution of E_0 in the interval I_0 . We evaluate $\text{var}(1/E_L)$ for $L = 20$ cm in a similar way by using assumptions about E_{20} and I_{20} . After exact integration (done analytically by **Maple**), the right-hand side of (4) becomes

$$2z + 2z^2(\exp(-1/z) - 1), \quad \text{where } z = L_{\text{corr}}/L,\quad (5)$$

an explicit function of L_{corr} and L . By using (5) and by fixing $L = 20$ cm, we can numerically solve (4) for L_{corr} .

As soon as $\text{var}(1/E_0)$ is inferred from the assumptions and L_{corr} is known from (4), we can use (4) to directly calculate $\text{var}(1/E_L)$ for $L = 80$ cm and the other bar lengths appearing in the truss structures. We assume that $\text{var}(1/E_{80})$ corresponds to either a uniform or normal distribution of E_{80} . Under these assumptions, we can infer I_{80} as either the entire range of a uniformly distributed random variable E_{80} or the 95% confidence interval of normally distributed random variable E_{80} , and check whether or not the validation data lie in I_{80} .

To obtain the vertical displacements δ_Q and δ_P , the axial elongation of the rods has to be combined with the bending of the transversally loaded beams, see [1] for details. The bending is expressed by the Green function technique. As a consequence, to compute the corresponding variance of the vertical displacements δ_Q and δ_P , integrals such as

$$\int_0^L \int_0^L \phi(x_1)\psi(x_2) \exp\left(-\frac{|x_1 - x_2|}{L_{\text{corr}}}\right) dx_1 dx_2\quad (6)$$

have to be evaluated. In the most complex setting of (6), ϕ and ψ are continuous piece-wise quadratic (in the accreditation experiment) or cubic (in the prediction

problem) functions. Again, **Maple** is able to analytically integrate expression (6). In a similar (but simpler) way, the respective means of δ_Q and δ_P can be calculated through the knowledge of $\int_0^L \phi(x_1)\psi(x_2) dx_1 dx_2$ and $\mathbf{E}[1/E_0]$.

Since we have made various assumptions, it will be useful to parametrize at least some of them to make the model partially parameter-dependent. By playing with the values of the parameters and by analyzing the model response, we hope to get at least some insight into the impact of uncertain inputs on the prediction problem truss behavior.

Let us define E_m as the mean of all the measured values of the Young modulus, that is E_0^y , E_{20}^y , and E_{80}^y taken together, twelve values in total. Let us introduce three fundamental parameters: E_{coef} , E_0^{ratio} , and $I_{20\text{-to-}I_0}$ ratio. The first parameter stands for a multiplicative coefficient that is used to control the centers of intervals I_0 , I_{20} , and I_{80} that are defined as coincident with $E_{\text{coef}}E_m$. The second parameter, E_0^{ratio} , is related to the distance between E_0^y (the measured values) and the ends of the interval I_0 that covers E_0^y . In detail, if I_c is the complement of I_0 in the set of real numbers, then $E_{\text{ratio}} = \text{dist}(I_c, E_0^y)/l_0$, where l_0 is the difference between the maximum and the minimum of the measured values E_0^y . Finally, the $I_{20\text{-to-}I_0}$ ratio is simply the ratio of the length of I_{20} to the length of I_0 .

Let us comment on Figure 2. The uppermost graph depicts the measured values E_0^y , E_{20}^y , and E_{80}^y (marked by \times) as well as the respective intervals I_0 , I_{20} , and I_{80} they are embedded in. Unlike I_0 and I_{20} , which are assumed, I_{80} is calculated from the

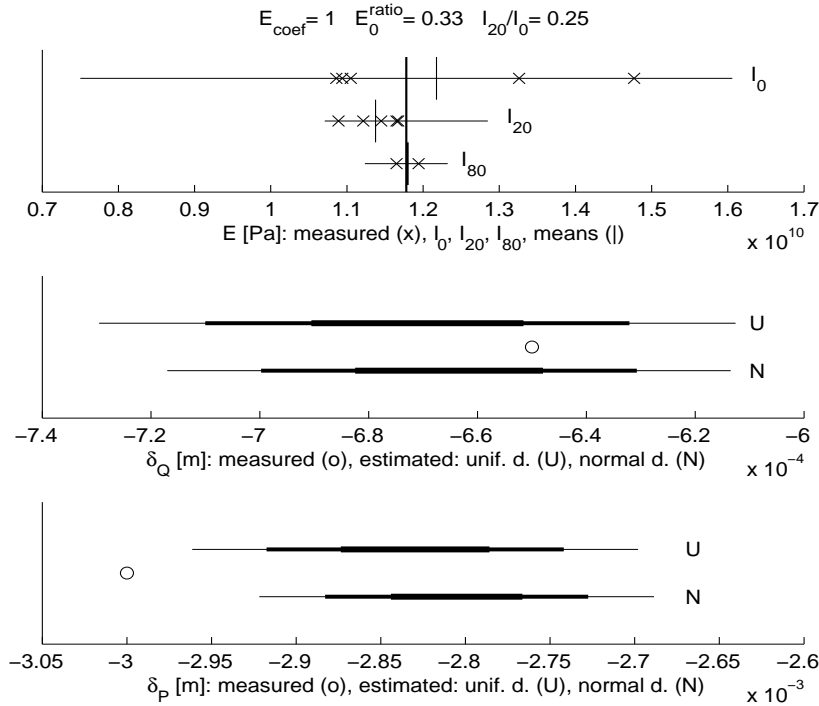


Fig. 2: Model outputs for fixed parameters.

assumptions and (4). Two intervals I_{80} should be depicted; one determined by the uniform distribution assumption, the other determined by the normal distribution assumption. Since, however, they almost coincide, only one line appears in the graph. The means of the measured values are marked by short vertical lines. The long vertical line marks the average value of the Young modulus we *assume* and calculate with, i.e., $E_{\text{coef}}E_m$. Note that E_{20}^v comprises five values but two of them almost coincide.

The middle graph shows the measured δ_Q marked by a small circle, and the estimated intervals for δ_Q constructed from the mean of δ_Q and the standard deviation of δ_Q inferred via the method outlined on the previous pages. The width of the lines marks the intervals determined by the mean and the first three multiples of (plus and minus) the standard deviation. Intervals stemming from the uniform (U, upper line) and normal (N, lower line) distribution of E_0 are drawn.

In Figure 2, the last graph is a parallel to the graph described in the previous paragraph, this time for δ_P , however. We see that the mean of δ_P is greater than the given acceptable limit of δ_P (-3 mm, marked by \circ). Indeed, it is more than three standard deviation values “on the safe side” even in the case of uniformly distributed Young modulus values.

Figure 3 shows what happens if we let the I_{20} -to- I_0 ratio change. In other words, we fix the interval encompassing the measured local Young moduli and we let the interval I_{20} get larger and larger. As a consequence, the inferred interval I_{80} becomes larger too, and the possible ranges of δ_Q and δ_P also increase. In Figure 3, the two thin lines depict E_{20}^{ratio} and E_{80}^{ratio} . These quantities have the meaning similar to that of E_0^{ratio} , but are defined by means of the pairs I_{20} , E_{20}^v , and I_{80} , E_{80}^v . The larger the ratio, the larger the distance between the measured values of the Young modulus and the ends on the respective intervals I_{20} and I_{80} . The two assumptions on the random variable distribution lead to two graphs of E_{80}^{ratio} . Since they almost coincide, only one line is depicted in Figure 3.

The “accreditation” dash and dash-dotted lines show the ratio of the distance between the measured δ_Q value and the calculated average of δ_Q to the standard deviation of δ_Q . Again, two assumed distributions of E are considered (u, uniform; n, normal).

The two thick lines that graph negative values depict the ratio of the difference between the limit displacement of -3 mm and the calculated average of δ_P to the standard deviation of δ_P . The uniform distribution assumption leads to a worse separation from the limit displacement than the normal distribution assumption. We observe that if the I_{20} -to- I_0 ratio increases, the distance between the set limit (-3 mm) and the calculated average decreases, that is, the probability that $\delta_P \leq -3$ mm increases.

The $*$ and \square symbols stem from the Chebyshev inequality [3, Section 33.10, inequality (3)], that is, they mark an upper bound on the probability that $\delta_P \leq -3$ mm; the estimates are multiplied by 10 in Figure 3. The values depend on the assumed distributions of E (u, uniform; n, normal).

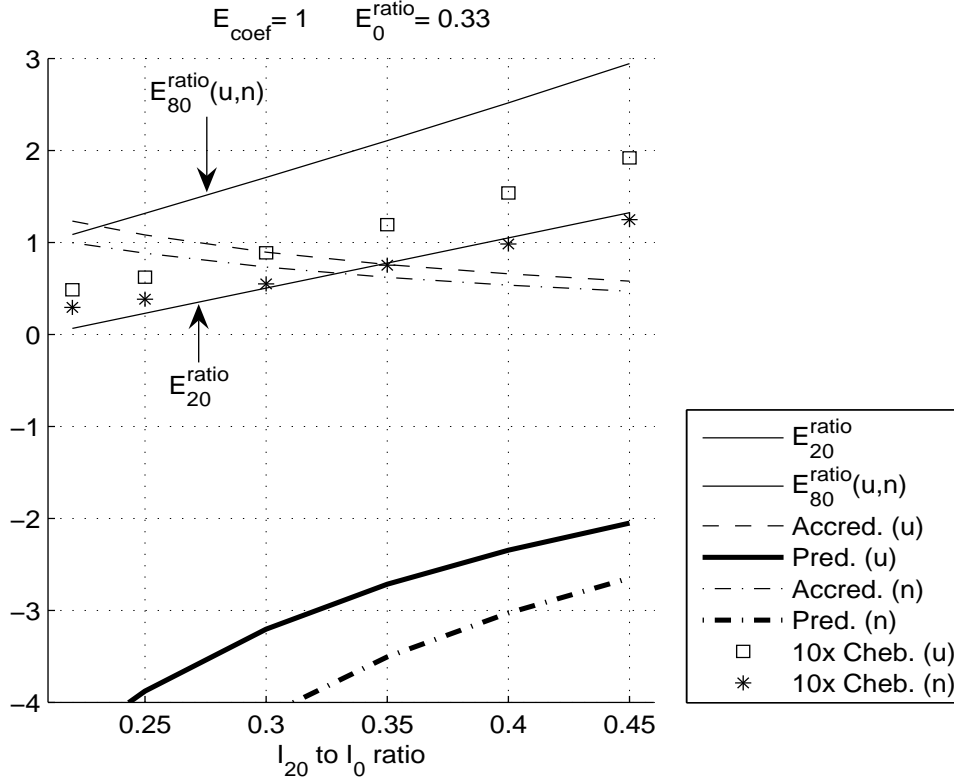


Fig. 3: Model outputs for variable parameters.

The graphs in Figure 2 and Figure 3 might indicate that the probability of reaching or exceeding the limit displacement in the prediction problem is sufficiently low even if we allow for rather large intervals to cover E_0^y and E_{20}^y . However, the graphs corresponding to perturbed values of E_{coef} (not displayed here) reveal a substantial sensitivity of outputs to the assumed average of the Young modulus. Its decrease ($E_{\text{coef}} = 0.98$, for instance) seems to be acceptable from the view of the measured data, but brings the predicted average displacement closer to the limit (less than three standard deviations). To make a more definite conclusion on the prediction problem solution, more data from measurements would be needed.

References

- [1] I. Babuška, F. Nobile, R. Tempone: *Model validation challenge problem: static frame problem*.
<http://www.esc.sandia.gov/VCWwebsite/MechanicsProblemDescrip.pdf>
- [2] S. Rahman, B.N. Rao: *An element-free Galerkin method for probabilistic mechanics and reliability*. Int. J. Solids Struct. **38**, 2001, 9313–9330.
- [3] K. Rektorys et al.: *Survey of applicable mathematics II*. Prometheus, Praha, 2000 (in Czech).